6-1-1992

# Control of Mechanical Systems With Rolling Constraints: Application to Dynamic Control of Mobile Robots

Nilanjan Sarkar
*University of Pennsylvania*

Xiaoping Yun
*University of Pennsylvania*

R. Vijay Kumar
*University of Pennsylvania*, kumar@grasp.upenn.edu



University of Pennsylvania Department of Computer and Information Science Technical Report No. MS-CIS-92-44.

# Control of Mechanical Systems With Rolling Constraints: Application to Dynamic Control of Mobile Robots


## Abstract

There are many examples of mechanical systems which require rolling contacts between two or more rigid bodies. Rolling contacts engender nonholonomic constraints in an otherwise holonomic system. In this paper, we develop a unified approach to the control of mechanical systems subject to both holonomic and nonholonomic constraints. We first present a state space realization of a constrained system and show that it is not input-state linearizable. We then discuss the input-output linearization and zero dynamics of the system. This approach is applied to the dynamic control of mobile robots. Two types of control algorithms for mobile robots are investigated: (a) trajectory tracking, and (b) path following. In each case, a smooth nonlinear feedback is obtained to achieve asymptotical input-output stability, and Lagrange stability of the overall system. Simulation results are presented to demonstrate the effectiveness of the control algorithms and to compare the performance of trajectory tracking and path following algorithms.



## Disciplines

Mechanical Engineering

## Comments

University of Pennsylvania Department of Computer and Information Science Technical Report No. MS-CIS-92-44.

# Control of Mechanical Systems with Rolling Constraints: Application to Dynamic Control of Mobile Robots

MS-CIS-92-44
GRASP LAB 320

Nilanjan Sarkar
Xiaoping Yun
Vijay Kumar

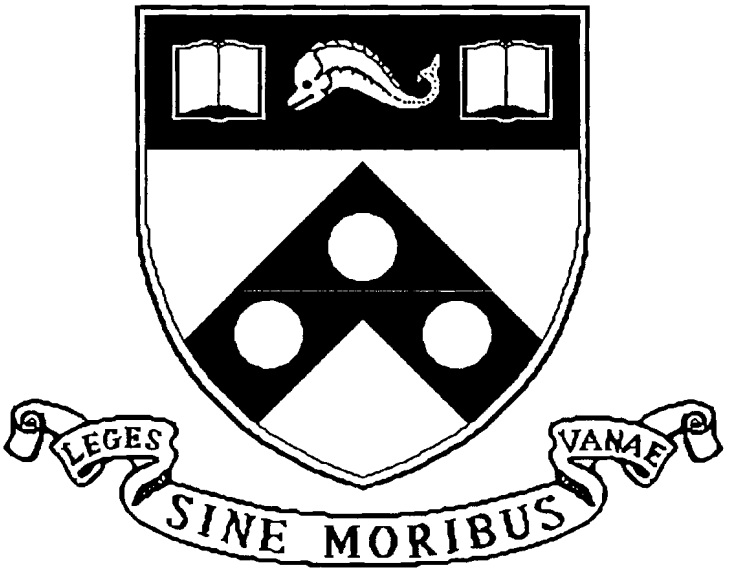


University of Pennsylvania
School of Engineering and Applied Science
Computer and Information Science Department
Philadelphia, PA 19104-6389

June 1992

# Control of Mechanical Systems with Rolling Constraints: Application to Dynamic Control of Mobile Robots

Nilanjan Sarkar, Xiaoping Yun, and Vijay Kumar
General Robotics and Active Sensory Perception (GRASP) Laboratory
University of Pennsylvania
3401 Walnut Street, Room 301C
Philadelphia, PA 19104-6228

**ABSTRACT**

There are many examples of mechanical systems which require rolling contacts between two or more rigid bodies. Rolling contacts engender nonholonomic constraints in an otherwise holonomic system. In this paper, we develop a unified approach to the control of mechanical systems subject to both holonomic and nonholonomic constraints. We first present a state space realization of a constrained system and show that it is not input-state linearizable. We then discuss the input-output linearization and zero dynamics of the system. This approach is applied to the dynamic control of mobile robots. Two types of control algorithms for mobile robots are investigated: (a) trajectory tracking, and (b) path following. In each case, a smooth nonlinear feedback is obtained to achieve asymptotical input-output stability, and Lagrange stability of the overall system. Simulation results are presented to demonstrate the effectiveness of the control algorithms and to compare the performance of trajectory tracking and path following algorithms.

# 1 Introduction

There are many examples of mechanical systems which require rolling contacts between two or more rigid bodies. These include wheeled vehicles such as conventional automobiles, unconventional actively coordinated robotic systems such as planetary rovers [11], manipulators grasping an object [25], and legged locomotion systems [12]. In this paper, the focus is on systems in which the rolling contact is maintained passively through external forces such as gravitational forces. This is true of almost all wheeled vehicles.

Rolling contacts between two rigid bodies engender nonholonomic constraints in an otherwise holonomic system. The control of constrained mechanical systems in the robotics literature has been mostly studied in the context of force control, and for the special case in which the contacts between a robot manipulator and its environment are modeled by holonomic constraints [24, 26]. The control of mechanical systems with nonholonomic constrained has only been studied very recently. Bloch and McClamroch [2] first demonstrated that a nonholonomic system cannot be stabilized to a single equilibrium point by a smooth feedback. They also showed that the system is small-time locally controllable [3]. Campion *et al.* [4] showed that the system is controllable regardless of the structure of nonholonomic constraints.

Wheeled mobile robots are typical examples of mechanical systems with nonholonomic constraints. Although navigation [10, 21] and planning [1, 14, 22, 9] of mobile robots have been investigated extensively over the past decade, the work on dynamic control of mobile robots with nonholonomic constraints is much more recent [6, 19, 7].

It is well known that the motion of a mechanical system may be described by a set of, say $n$, generalized coordinates and differential equations of motion relating the coordinates to external forces and moments. If the system is subject to, say $m$, holonomic constraints, $m$ of the generalized coordinates may be eliminated from the motion equations, although the elimination process is often cumbersome. This results in a reduced order for the motion equations [17]. The state space representation is quite simple and the analysis and design of controllers for such a mechanical system is well understood and documented. On the other hand, if the system is subject to say $k$ nonholonomic constraints, the number of generalized coordinates can not be reduced by $k$. Therefore, before well-known state space based control methods can be employed, an alternative approach is necessary to represent the motion and constraint equations in the state space.

In this paper, we present a unified approach to the control of mechanical systems subject to both holonomic and nonholonomic constraints. We first characterize the constrained systems in the state space and formulate the control problem of such systems as a standard nonlinear system control problem. We show that the systems are not input-state linearizable if at least one of the constraints is nonholonomic. Since the state of the systems can not be made asymptotically stable by smooth feedback, we pursue feedback control methods which achieve asymptotical input-output stability.

Applying the control methods to dynamic control of mobile robots, we discuss two broad categories of output equations. In the first category the output vector consists of a subset, say $p$, of a set of generalized coordinates. Thus the system is designed to follow a desired trajectory, $p^d(t)$ where t is the time. This is called *trajectory tracking* in this paper. In the other category, the history $p^d(t)$ is not as important as the path, $p^d(s)$. Here $s$ is any convenient parameter (say an arc-length variable) that parametrizes the path. The trajectory tracking control scheme is shown in Figure 1 (a) for a vehicle subject to nonholonomic constraints[1]. The desired path is a straight line

[1]The theory and the details of implementation are discussed in the following sections.

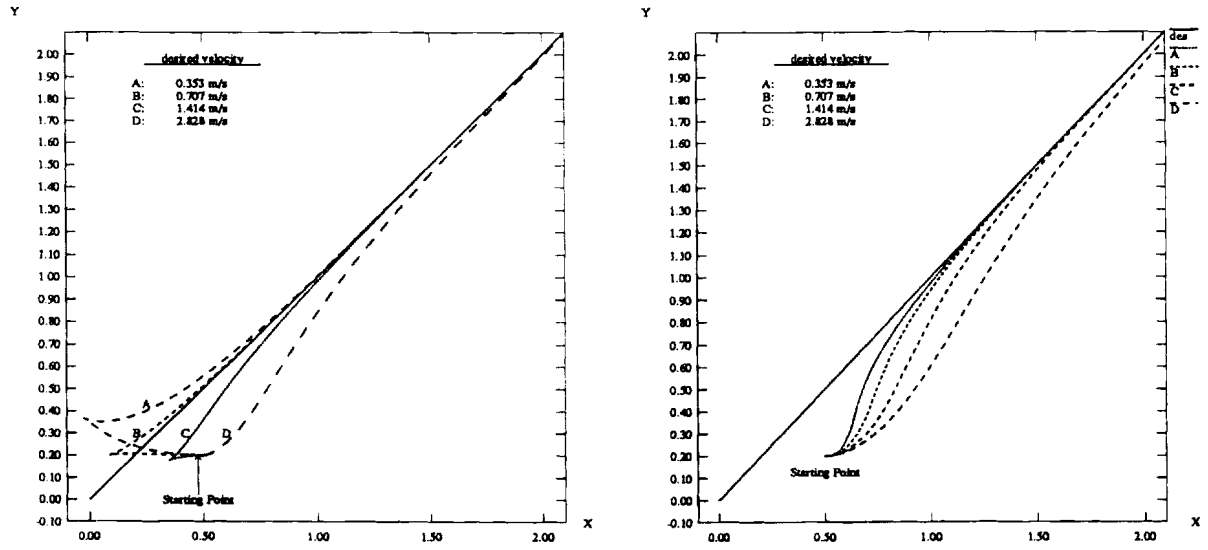


Figure 1: (a) Trajectories and (b) paths for the geometric center $P_o$.

and the initial position is not on the path. The locus of a reference point on the vehicle is shown in the figure for different desired forward velocities. By forward velocity we mean the component of the velocity of the reference point perpendicular to the axis of the wheels in a preferred "forward" direction. If a trajectory tracking control algorithm is employed, the path of the reference point is not a "smooth merge". It is possible that the vehicle may first go in one direction and then the opposite direction depending on the definition of $p^d(t)$. While this may be acceptable and even desirable for some applications, for road following or path following, the paths shown in Figure 1 (b) is more appropriate[2]. Here the desired output is specified in terms of the path $p^d(s)$ and the speed along the path, $\dot{s}$. This is termed *dynamic path following* in this paper.

For each case, we develop a nonlinear feedback which realizes the input-output linearization and input-output decoupling. At the same time, we show that the zero dynamics of the system is Lagrange stable. A computer simulation of a mobile robot is used to study the control of mechanical systems with rolling contacts. Both types of control schemes are investigated through numerical experiments and their performances are compared. It is concluded that a dynamic path-following scheme is more appropriate for vehicle control applications.

# 2 Theoretic Formulation

## 2.1 Dynamic Equations of Motion

Consider a mechanical system with $n$ generalized coordinates $q$ subject to $m$ bilateral constraints which are in the form

$$C(q, \dot{q}) = 0 \tag{1}$$

If a constraint equation is in the form $C_i(q) = 0$, or can be integrated into this form, it represents a holonomic constraint. Otherwise it represents a kinematic (as opposed to a geometric) constraint

[2] a more exhaustive study follows in Section 4

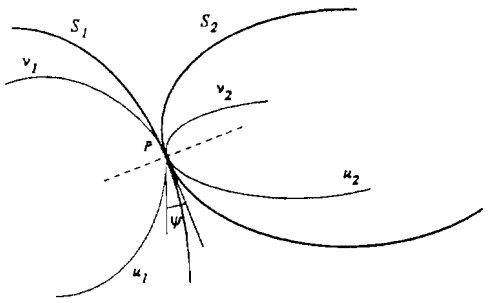


Figure 2: Two Rigid Bodies in Contact

and is termed nonholonomic.

We assume that we have $k$ holonomic and $m-k$ nonholonomic independent constraints, all of which can be written in the form

$$A(q)\dot{q} = 0 \tag{2}$$

where $A(q)$ is an $m \times n$ full-rank matrix . Let $s_1(q), \cdots, s_{n-m}(q)$ be a set of smooth and linearly independent vector fields in $\mathcal{N}(A)$, the null space of $A(q)$, *i.e.*,

$$A(q)s_i(q) = 0 \qquad i = 1, \ldots, n-m.$$

Let $S(q)$ be the full rank matrix made up of these vectors

$$S(q) = [s_1(q) \quad \cdots \quad s_{n-m}(q)] \tag{3}$$

and let $\Delta$ be the distribution spanned by these vector fields

$$\Delta = span\{s_1(q), \quad \cdots, \quad s_{n-m}(q)\}$$

It follows that $\dot{q} \in \Delta$. $\Delta$ may or may not be involutive. For that reason, we let $\Delta^*$ be the smallest involutive distribution containing $\Delta$. It is clear that $dim(\Delta) \leq dim(\Delta^*)$. There are three possible cases (as observed by Campion, *et al.* in [4]). First, if $k = m$, that is, all the constraints are holonomic, then $\Delta$ is involutive itself. Second, if $k = 0$, that is, all the constraints are nonholonomic, then $\Delta^*$ spans the entire space. Finally, if $0 < k < m$, the $k$ constraints are integrable and $k$ components of the generalized coordinates may be eliminated from the motion equations. In this case, $dim(\Delta^*) = n - k$.

## 2.2 Contact Between Rigid Bodies

### 2.2.1 Spatial Case

Consider two bodies in contact at a point $P$, as shown in Figure 2. We use $S_1$ and $S_2$ to denote the surfaces of the two bodies, respectively. Let $S_{1P}$ be an open and connected subset of $S_1$ containing the point $P$. Then the pair $(f_1, U_1)$ is called a coordinate system of $S_{1P}$ if there exists an open subset $U_1$ of $\mathbf{R}^2$ and an invertible map $f_1 : U_1 \longrightarrow S_{1P}$ such that the partial derivatives $\frac{\partial f_1(\mathbf{u})}{\partial u_1}$ and $\frac{\partial f_1(\mathbf{u})}{\partial v_1}$ are linearly independent for all $\mathbf{u} = (u_1, v_1) \in U_1$. We choose an orthogonal coordinate

system so that the metric tensor is diagonal. Let $M_1$ be the square root of the metric tensor for $S_1$ at point $P$ in the coordinate system $(f_1, U_1)$.

All the notation for $S_2$ can be defined similarly. The contact point on $S_1$ (or $S_2$) is specified by the coordinates $u_1$ and $v_1$ (or $u_2$ and $v_2$). In order to completely specify the contact configuration we need a fifth variable $\psi$, which can be the angle between the tangent to the $u_1$-coordinate curve and that to the $u_2$-coordinate curve at the contact point, measured about the outward-pointing normal to $S_1$. Thus

$$q = [u_1 \quad v_1 \quad u_2 \quad v_2 \quad \psi]^T \tag{4}$$

constitutes a set of generalized coordinates.

Let $(v_x, v_y, v_z)$ be the velocity of the point $p$ on $S_2$ relative to the point $p$ on $S_1$, and $(\omega_x, \omega_y, \omega_z)$ the angular velocity of $S_2$ relative to $S_1$. The contact kinematic equations have been derived by Montana [15]. For rolling contact, since $v_x = 0$ and $v_y = 0$, we obtain the rolling constraint equation [27]

$$R_\psi M_1 \dot{\mathbf{u}}_1 - M_2 \dot{\mathbf{u}}_2 = 0 \tag{5}$$

where

$$R_\psi = \begin{bmatrix} \cos\psi & -\sin\psi \\ -\sin\psi & -\cos\psi \end{bmatrix}$$

It can be rewritten in the form of Equation (2) if

$$A(q) = [R_\psi M_1 \quad -M_2 \quad 0]$$

We choose the $S(q)$ matrix (defined in Equation (3)) as follows:

$$S(q) = [s_1(q) \quad s_2(q) \quad s_3(q)] = \begin{bmatrix} 1 & 0 & 0 \\ 0 & 1 & 0 \\ s_{31} & s_{32} & 0 \\ s_{41} & s_{42} & 0 \\ 0 & 0 & 1 \end{bmatrix} \tag{6}$$

where

$$\begin{bmatrix} s_{31} & s_{32} \\ s_{41} & s_{42} \end{bmatrix} = M_2^{-1} R_\psi M_1$$

We now compute the Lie brackets

$$s_4(q) = [s_1(q), s_3(q)] = [0 \quad 0 \quad s_{34} \quad s_{44} \quad 0]^T$$

$$s_5(q) = [s_2(q), s_3(q)] = [0 \quad 0 \quad s_{35} \quad s_{45} \quad 0]^T$$

where

$$\begin{bmatrix} s_{34} & s_{35} \\ s_{44} & s_{45} \end{bmatrix} = -M_2^{-1} \frac{\partial R_\psi}{\partial \psi} M_1$$

Therefore, the distribution spanned by the vector fields $s_1(q)$, $s_2(q)$, and $s_3(q)$ is not involutive since $s_4(q)$ and $s_5(q)$ are not in the distribution. Further, $s_1(q)$ through $s_5(q)$ span the entire 5-dimensional configuration space. It follows that the two rolling constraints are nonholonomic. Note that for pure rolling, that is, if the spin motion $\omega_z = 0$ in addition to $v_x$ and $v_y$ being zero, a similar approach shows that all three constraints are nonholonomic.

### 2.2.2 Planar Case

$U_1$ and $U_2$ are now open subsets of $\mathbf{R}$ and the contact configuration is specified by two coordinates $q = [u_1 \quad u_2]^T$. The kinematic equations of rolling contact, Equation (5) reduces to

$$M_1 \dot{u}_1 - M_2 \dot{u}_2 = 0 \tag{7}$$

where $M_i = \frac{\partial f_i}{\partial u_i}$. The $A(q)$ matrix is clearly

$$A(q) = [M_1 \quad -M_2]$$

and the $S(q)$ matrix, which spans the null space of $A(q)$, is $S(q) = [M_2 \quad M_1]^T$. The distribution spanned by $S(q)$, a single vector field, is trivially involutive. Therefore we get the well-known result that the rolling constraint for the planar case is holonomic.

## 2.3 State Space Representation

We now consider the mechanical system with constraints given by (2), whose equations of motion are described by

$$M(q)\ddot{q} + V(q,\dot{q}) = E(q)\tau - A^T(q)\lambda \tag{8}$$

where $M(q)$ is the $n \times n$ inertia matrix, $V(q,\dot{q})$ is the vector of position and velocity dependent forces, $E(q)$ is the $n \times r$ input transformation matrix[3], $\tau$ is the $r$-dimensional input vector, $A(q)$ as in Equation (2) is the $m \times n$ Jacobian matrix, and $\lambda$ is the vector of constraint forces.

We allow for $k$ of the $m$ constraints in Equation (2) to be holonomic. Since the constrained velocity is always in the null space of $A(q)$, it is possible to define $n-m$ velocities $\nu(t) = [\nu_1 \quad \nu_2 \cdots \nu_{n-m}]$ such that

$$\dot{q} = S(q)\nu(t) \tag{9}$$

These velocities need not be integrable but they can be regarded as being time derivatives of $n-m$ *quasi-coordinates* $\mu_1, \mu_2, \ldots, \mu_{n-m}$ [17]. For example, we can choose the quasi-coordinates so that $\nu = \dot{\mu} = S^+\dot{q}$, where $S^+$ is a generalized inverse of $S$.

Differentiating Equation (9), substituting the expression for $\ddot{q}$ into (8), and premultiplying by $S^T$, we have

$$S^T(MS\dot{\nu}(t) + M\dot{S}\nu(t) + V) = S^T E\tau \tag{10}$$

Note that since $S \in \mathcal{N}(A)$, $S^T A^T \lambda$ vanishes in this equation.

Using the state space variable $x = [q^T \quad \nu^T]^T$, we have

$$\dot{x} = \begin{bmatrix} S\nu \\ f_2 \end{bmatrix} + \begin{bmatrix} 0 \\ (S^TMS)^{-1}S^TE \end{bmatrix} \tau \tag{11}$$

where $f_2 = (S^TMS)^{-1}(-S^TM\dot{S}\nu - S^TV)$. Assuming that the number of actuator inputs is greater than or equal to the number of the degrees of freedom of the mechanical system ($r \geq n-m$), and $(S^TMS)^{-1}S^TE$ has rank $n-m$, we may apply the following nonlinear feedback[4]

[3] $E(q)$ is an identity matrix in most cases. However, if the generalized coordinates are chosen to be some variables other than the joint variables, or if there are passive joints without actuators, it is not an identity matrix.

[4] While it is convenient to use the generalized inverse to resolve the redundancy, it is productive to use surplus inputs to control the interaction forces and moments [28, 13]. In this paper, for the most part,we will not be concerned with redundant systems.

$$\tau = ((S^T M S)^{-1} S^T E)^+ (u - f_2) \tag{12}$$

The state equation simplifies to the form

$$\dot{x} = f(x) + g(x)u \tag{13}$$

where

$$f(x) = \begin{bmatrix} S(q)\nu \\ 0 \end{bmatrix}, \quad g(x) = \begin{bmatrix} 0 \\ I \end{bmatrix}.$$

## 2.4 Control Properties

The following two properties of the system (13) have been established in [4] for the special case in which *all* constraints are nonholonomic.

**Theorem 1** *The nonholonomic system (13) is controllable.*

**Theorem 2** *The equilibrium point $x = 0$ of the nonholonomic system (13) can be made Lagrange stable, but can not be made asymptotically stable by a smooth state feedback.*

In the rest of this section, we discuss the more general case in which Equation (2) consists of both holonomic and nonholonomic constraints.

**Theorem 3** *The system in Equation (13) is not input-state linearizable by a state feedback if one or more constraints are nonholonomic.*

**Proof:** The system has to satisfy two conditions in order to be input-state linearizable: the strong accessibility condition and the involutivity condition [16, p. 179]. It is shown below that the involutivity condition is not satisfied.

Define a sequence of distributions

$$D_j = span\{L_f^i g \mid i = 0, 1, \ldots, j-1\}, \quad j = 1, 2, \ldots$$

Then the involutivity condition requires that the distributions $D_1$, $D_2$, ..., $D_{2n-m}$ are all involutive. Note that the dimension of the state variable is $2n - m$. $D_1 = span\{g\}$ is involutive since $g$ is constant. Next we compute

$$L_f g = [f, g] = \frac{\partial g}{\partial x} f - \frac{\partial f}{\partial x} g = - \begin{bmatrix} S(q) \\ 0 \end{bmatrix}$$

Since the distribution $\Delta$ spanned by the columns of $S(q)$ is not involutive, the distribution $D_2 = span\{g, L_f g\}$ is not involutive. Therefore, the system is not input-state linearizable. □

Although a system with nonholonomic constraints is not input-state linearizable, it may be input-output linearizable if a proper set of output equations are chosen. Consider the position control of the system, *i.e.*, the output equations are functions of position state variable $q$ only. Since the number of the degrees of freedom of the system is instantaneously $n - m$, we may have at most $n - m$ independent position outputs equations.

$$y = h(q) = [h_1(q) \quad \cdots \quad h_{n-m}(q)] \tag{14}$$

The necessary and sufficient condition for input-output linearization is that the decoupling matrix has full rank [16]. With the output equation (14), the decoupling matrix $\Phi(x)$ for the system is the $(n-m) \times (n-m)$ matrix

$$\Phi(q) = J_h(q)S(q) \tag{15}$$

where $J_h = \frac{\partial h}{\partial q}$ is the $(n-m) \times n$ Jacobian matrix. $\Phi(x)$ is nonsingular if the rows of $J_h$ are independent of the rows of $A(q)$.

To characterize the zero dynamics and achieve input-output linearization, we introduce a new state space variable $z$ defined as follows

$$z = T(x) = \begin{bmatrix} z_1 \\ z_2 \\ z_3 \end{bmatrix} = \begin{bmatrix} h(q) \\ L_f h(q) \\ \tilde{h}(q) \end{bmatrix} = \begin{bmatrix} h(q) \\ \Phi(q)\nu \\ \tilde{h}(q) \end{bmatrix} \tag{16}$$

where $\tilde{h}(q)$ is an m-dimensional function such that $[J_h^T \quad J_{\tilde{h}}^T]$ has full rank. It is easy to verify that $T(x)$ is indeed a diffeomorphism [27] and thus a valid state space transformation. The system under the new state variable $z$ is characterized by

$$\dot{z}_1 = \frac{\partial h}{\partial q}\dot{q} = z_2 \tag{17}$$

$$\dot{z}_2 = = \dot{\Phi}(q)\nu + \Phi(q)u \tag{18}$$

$$\dot{z}_3 = J_{\tilde{h}} S\nu = J_{\tilde{h}} S (J_h S)^{-1} z_2 \tag{19}$$

Utilizing the following state feedback

$$u = \Phi^{-1}(q)(v - \dot{\Phi}(q)\nu) \tag{20}$$

we achieve input-output linearization as well as input-output decoupling by noting the observable part of the system

$$\dot{z}_1 = z_2 \qquad \dot{z}_2 = v \qquad y = z_1$$

The zero dynamics of the system is (obtained by substituting $z_1 = 0$ and $z_2 = 0$) [23]

$$\dot{z}_3 = 0 \tag{21}$$

which is clearly Lagrange stable but not asymptotically stable.

# 3 Dynamics and Control of a Mobile Platform

## 3.1 Constraint Equations

In order to illustrate the methodology, we consider a mobile robot similar to the LABMATE[5] mobile platform. It has two driving wheels on an axis which passes through the vehicle geometric center as shown in Figure 3. They are powered by D.C. motors. The platform has four passive wheels (castors) on each corner.

The following notation will be used in the paper (see Figure 4).

[5]LABMATE is a trdeamark of Transition Research Corporation.

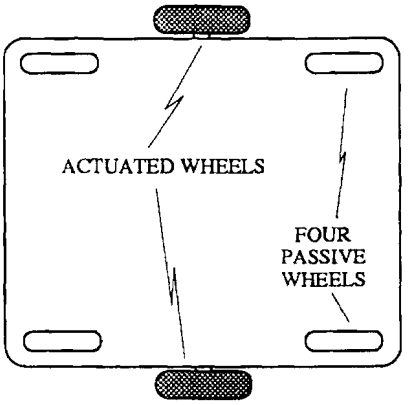


Figure 3: An example of a wheeled platform (top view)

| | |
|---|---|
| $x$–$y$: | the world coordinate system; |
| $X$–$Y$: | the coordinate system fixed to the cart as shown in Figure 4; |
| $P_o$: | the geometric center with coordinates ($x_o$, $y_o$) which is the intersection of the axis of symmetry with the driving wheel axis; |
| $P_c$: | the center of mass of the platform with coordinates ($x_c$, $y_c$); |
| $P_l$: | a virtual reference point attached to the platform with coordinates ($x_l$, $y_l$); |
| $b$: | the distance between either driving wheel and the axis of symmetry; |
| $r$: | the radius of each driving wheel; |
| $m_c$: | the mass of the platform without the driving wheels and the rotors of the DC motors; |
| $m_w$: | the mass of each driving wheel plus the rotor of its motor; |
| $I_c$: | the moment of inertia of the platform without the driving wheels and the rotors of the motors about a vertical axis through $P_c$; |
| $I_w$: | the moment of inertia of each wheel and the motor rotor about the wheel axis; |
| $I_m$: | the moment of inertia of each wheel and the motor rotor about a wheel diameter; |
| $a$: | the length of the platform in the direction perpendicular to the driving wheel axis; |
| $d$: | the distance from $P_o$ to $P_c$ along the positive $X$-axis. |

If we ignore the passive wheels, the configuration of the platform can be described by five generalized coordinates. These are the three variables that describe the position and orientation of the platform and two variables that specify the angular positions for the driving wheels. Therefore, let

$$q = (x_c, y_c, \phi, \theta_r, \theta_l)$$

where $(x_c, y_c)$ is the coordinates of the center of mass $P_c$ in the world coordinate system, and $\phi$ is the heading angle of the platform as shown in Figure 4. $\theta_r$ and $\theta_l$ are the angular positions of the right and left driving wheels respectively.

Assuming the driving wheels roll (and do not slip) there are three constraints. First, the velocity of the point $P_o$ of the platform must be in the direction of the axis of symmetry, the X-axis:

$$\dot{y}_c \cos\phi - \dot{x}_c \sin\phi - \dot{\phi}\, d = 0 \tag{22}$$

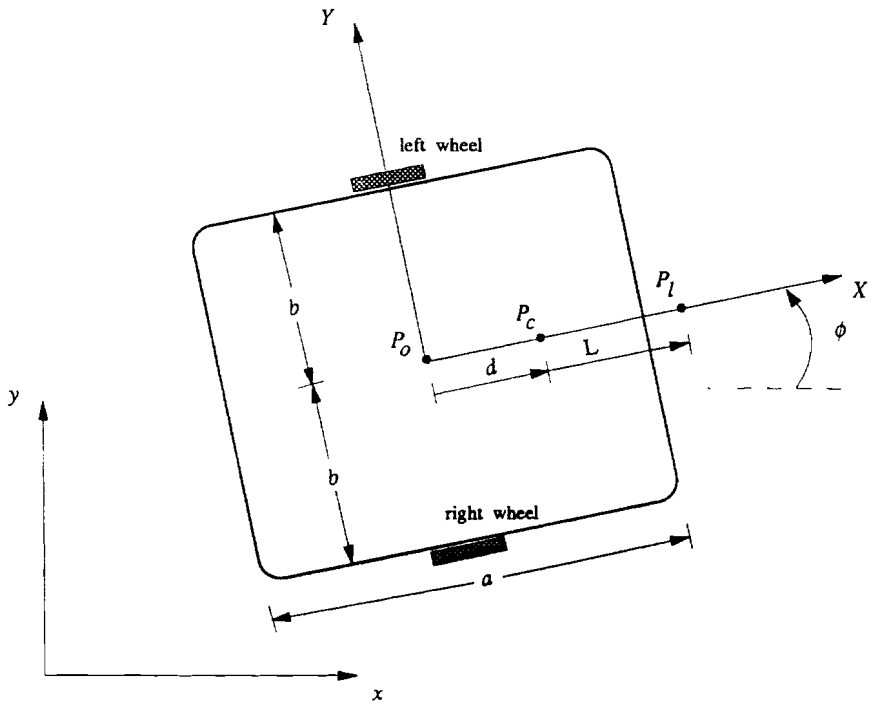


Figure 4: Notation for the geometry of the mobile platform

Further, if the driving wheels do not slip,

$$\dot{x}_c \cos\phi + \dot{y}_c \sin\phi + b\dot{\phi} = r\dot{\theta}_r \tag{23}$$

$$\dot{x}_c \cos\phi + \dot{y}_c \sin\phi - b\dot{\phi} = r\dot{\theta}_l \tag{24}$$

The three constraints can be written in the form:

$$A(q)\dot{q} = 0$$

where

$$A(q) = \begin{bmatrix} -\sin\phi & \cos\phi & -d & 0 & 0 \\ -\cos\phi & -\sin\phi & -b & r & 0 \\ -\cos\phi & -\sin\phi & b & 0 & r \end{bmatrix} \tag{25}$$

Thus the mechanical system has two degrees of freedom.

It is straightforward to verify that the following matrix

$$S(q) = [s_1(q),\ s_2(q)] = \begin{bmatrix} c(b\cos\phi - d\sin\phi) & c(b\cos\phi + d\sin\phi) \\ c(b\sin\phi + d\cos\phi) & c(b\sin\phi - d\cos\phi) \\ c & -c \\ 1 & 0 \\ 0 & 1 \end{bmatrix}$$

satisfies $A(q)S(q) = 0$, where the constant $c = \frac{r}{2b}$. Computing the Lie bracket of $s_1(q)$ and $s_2(q)$ we obtain

$$s_3(q) = [s_1(q),\ s_2(q)] = \begin{bmatrix} -rc\sin\phi \\ rc\cos\phi \\ 0 \\ 0 \\ 0 \end{bmatrix}$$

which is not in the distribution $\Delta$ spanned by $s_1(q)$ and $s_2(q)$. Therefore, at least one of the constraints is nonholonomic. We continue by computing the Lie bracket of $s_1(q)$ and $s_3(q)$

$$s_4(q) = [s_1(q),\ s_3(q)] = \begin{bmatrix} -rc^2\cos\phi \\ -rc^2\sin\phi \\ 0 \\ 0 \\ 0 \end{bmatrix}$$

which is linearly independent of $s_1(q)$, $s_2(q)$, and $s_3(q)$. However, we can verify that the distribution spanned by $s_1(q)$, $s_2(q)$, $s_3(q)$ and $s_4(q)$ is involutive. Therefore, we have

$$\Delta^* = span\{s_1(q),\ s_2(q),\ s_3(q),\ s_4(q)\} \tag{26}$$

It follows that, among the three constraints, two of them are nonholonomic and the third one is holonomic. To obtain the holonomic constraint, we subtract Equation (24) from Equation (23).

$$2b\dot{\phi} = r(\dot{\theta}_r - \dot{\theta}_l) \tag{27}$$

Integrating the above equation we have

$$\phi = c(\theta_r - \theta_l) + c_1 \tag{28}$$

where $c_1$ is a constant of integration. This is clearly a holonomic constraint equation. Note that $\phi$, $\theta_r$ and $\theta_l$ can be defined in such a way that $c_1$ may be taken to be zero.

### 3.2 Dynamic Equations

We now derive the dynamic equation for the mobile platform. The Lagrange equations of motion of the platform with the Lagrange multipliers $\lambda_1$, $\lambda_2$, and $\lambda_3$ are given by

$$m\ddot{x}_c + 2m_w d(\ddot{\phi}\sin\phi + \dot{\phi}^2\cos\phi) - \lambda_1\sin\phi - (\lambda_2+\lambda_3)\cos\phi = 0 \tag{29}$$

$$m\ddot{y}_c - 2m_w d(\ddot{\phi}\cos\phi - \dot{\phi}^2\sin\phi) + \lambda_1\cos\phi - (\lambda_2+\lambda_3)\sin\phi = 0 \tag{30}$$

$$2m_w d(\ddot{x}_c\sin\phi - \ddot{y}_c\cos\phi) + I\ddot{\phi} - d\lambda_1 + b(\lambda_3 - \lambda_2) = 0 \tag{31}$$

$$I_w\ddot{\theta}_r + \lambda_2 r = \tau_r \tag{32}$$

$$I_w\ddot{\theta}_l + \lambda_3 r = \tau_l \tag{33}$$

where

$$\begin{aligned} m &= m_c + 2m_w \\ I &= I_c + 2m_w(d^2+b^2) + 2I_m \end{aligned}$$

and $\tau_r$ and $\tau_l$ are the torques acting on the wheel axis generated by the right and left motors respectively. These five equations of motion can easily be written in the form of Equation (8). The matrices $M(q)$, $V(q,\dot{q})$, and $E(q)$ are given by:

$$M(q) = \begin{bmatrix} m & 0 & 2m_w d\sin\phi & 0 & 0 \\ 0 & m & -2m_w d\cos\phi & 0 & 0 \\ 2m_w d\sin\phi & -2m_w d\cos\phi & I & 0 & 0 \\ 0 & 0 & 0 & I_w & 0 \\ 0 & 0 & 0 & 0 & I_w \end{bmatrix}$$

$$V(q,\dot{q}) = \begin{bmatrix} 2m_w d\dot{\phi}^2\cos\phi \\ 2m_w d\dot{\phi}^2\sin\phi \\ 0 \\ 0 \\ 0 \end{bmatrix} \qquad E(q) = \begin{bmatrix} 0 & 0 \\ 0 & 0 \\ 0 & 0 \\ 1 & 0 \\ 0 & 1 \end{bmatrix} \qquad \tau = \begin{bmatrix} \tau_r \\ \tau_l \end{bmatrix}$$

If we choose $\theta_r$ and $\theta_l$ to be the two quasi-cordinates,

$$\nu = \begin{bmatrix} \nu_1 \\ \nu_2 \end{bmatrix} = \begin{bmatrix} \dot{\theta}_l \\ \dot{\theta}_r \end{bmatrix}$$

and we can verify that Equation 9 is satisfied. Then the state variable is the following vector:

$$x = [x_c \quad y_c \quad \phi \quad \theta_l \quad \theta_r \quad \dot{\theta}_l \quad \dot{\theta}_r]^T$$

Using this state variable, the dynamics of the mobile platform can be represented in the state space form, Equation (11).

### 3.3 Output Equations

While the state equations of a dynamic system are uniquely determined by its dynamic characteristics, the output variables are chosen in such a way that the tasks to be performed by the dynamic system can be *conveniently specified* and the controller design can be *easily accomplished.* For example, if a six degree-of-freedom robot manipulator is to perform pick-and-place or trajectory tracking tasks, the six-dimensional joint position vector or the six-dimensional Cartesian position and orientation vector is normally chosen as the output vector. In this section, we present a number of possible choices for output variables of the control system for the mobile platform and discuss each case.

Let $P_l$ be the reference point on the mobile platform. We choose $P_l$ to be a virtual point on the axis of symmetry displaced through a distance $L$ from the center of mass $P_c$ as shown in Figure 4 ($L$ can be positive, negative, or zero). Its coordinates are denoted by $(x_l, y_l)$:

$$x_l = x_c + L\cos\phi \tag{34}$$

$$y_l = y_c + L\sin\phi \tag{35}$$

Since the system has two inputs, we may choose any two output variables. We consider the following four types of output equations:

**Type I:** $y = h(q) = [x_l \quad y_l]^T$
**Type II:** $y = h(q) = [x_l \quad \phi]^T$
**Type III:** $y = h(q) = [y_l \quad \phi]^T$
**Type IV:** $y = h(x) = [h_1(q) \quad h_2(\nu)]^T$

The Type I output equation results in a trajectory tracking control system which has been studied in [6, 19]. The corresponding decoupling matrix for this output is

$$\Phi(q) = J_h(q)S(q) = \begin{bmatrix} \Phi_{11} & \Phi_{12} \\ \Phi_{21} & \Phi_{22} \end{bmatrix} \tag{36}$$

where

$$\Phi_{11} = c(b\cos\phi - (d+L)\sin\phi) \tag{37}$$
$$\Phi_{12} = c(b\cos\phi + (d+L)\sin\phi) \tag{38}$$
$$\Phi_{21} = c(b\sin\phi + (d+L)\cos\phi) \tag{39}$$
$$\Phi_{21} = c(b\sin\phi - (d+L)\cos\phi) \tag{40}$$

Since the determinant of the decoupling matrix is $\det(\Phi(q)) = -\frac{r^2(d+L)}{2b}$, it is singular if and only if $L = -d$, that is, if point $P_l$ coincides with point $P_o$. Therefore, trajectory tracking of the point $P_o$ is not possible as pointed out in [19]. This is clearly due to the presence of nonholonomic constraints. Choosing $L$ not equal to $-d$, we may decouple and linearize the system as follows. The derivative of the decoupling matrix is (noting that $\Phi$ is a function of $\phi$ only)

$$\dot{\Phi}(q) = \frac{d\Phi}{d\phi}\dot{\phi} = \frac{d\Phi}{d\phi}c(\nu_1 - \nu_2)$$

Since $S^T E = I_{2\times 2}$, the nonlinear feedback (Equations (12) and (20)) in this case simplifies to

$$\tau = (S^T M S)u + S^T M \dot{S}\nu + S^T V \tag{41}$$

and

$$u = \Phi^{-1}(q)(v - \dot{\Phi}(q)\nu) \tag{42}$$

The linearized and decoupled subsystems are

$$\ddot{y}_1 = v_1 \tag{43}$$
$$\ddot{y}_2 = v_2 \tag{44}$$

Type II and Type III systems are similar. For a Type II output equation, the decoupling matrix is

$$\Phi_{II}(q) = J_h(q)S(q) = \begin{bmatrix} \Phi_{11} & \Phi_{12} \\ c & -c \end{bmatrix} \tag{45}$$

where $\Phi_{11}$ and $\Phi_{12}$ are defined by Equations (37) and (38). Its determinant is $\det(\Phi_{II}(q)) = -2c^2 b\cos\phi$. $\Phi_{II}$ is nonsingular if $\cos\phi \neq 0$. Similarly, the decoupling matrix for Type III output is nonsingular if $\sin\phi \neq 0$. Thus, it is possible to decouple and linearize the system with Type II and Type III outputs in a large region of the state space. However, it is not convenient to specify control tasks with these two types of outputs. We discuss Type IV output equations and the *dynamic path following problem* in the next section below.

### 3.4 Dynamic Path Following

If we analyze automobile manoeuvring, the two most important requirements are to follow the road (or path) by staying as close to the path as possible and to maintain the desired forward velocity. With this in mind, we would like to choose an output equation with two variables: the shortest distance of a reference point on the mobile platform from the desired path and the forward velocity. By doing so, we formulate a dynamic path following problem [20] instead of a trajectory tracking problem. In a trajectory tracking problem, the desired time history of the output variables is specified. Therefore, in this case, the task is not only to reach a point but also to reach it at a specified time instant. In a path following problem, however, the geometry of the path is specified. In this case, it is more important to follow the path closely than to reach points on the path at specified time instants. By specifying the desired forward velocity, we (indirectly) ensure that the vehicle reaches desired points on the path.

In this section, we achieve path following by appropriately choosing $h_1$ and $h_2$. $h_1$ is defined as the shortest distance from the point $P_l$ on the mobile platform to the desired path. The formulation is quite general since $P_l$ can be anywhere on the vehicle, although we prefer to choose $P_l$ on the $X$-axis. However, note that for an arbitrary path, there is no closed form expression for the shortest distance from $P_l$ to the path. We define $h_2$ to be the component of the velocity of $P_l$ along the $X$-axis. We call this the forward velocity.

We first consider two basic paths: a straight line path and a circular path. A closed form expression for the distance from a point to the path can be easily obtained in either case.

We first consider a circular path. Let $P_f$ be the center of the circular path whose coordinates are denoted by $(x_f, y_f)$ in the world coordinate system. Let $R$ be the radius of the circular path. We choose $h_1$ as follows:

$$h_1(q) = h_1(x_c, y_c, \phi) = ((x_l - x_f)^2 + (y_l - y_f)^2)^{1/2} - R \tag{46}$$

Note that the shortest distance from point $P_l$ to the circular path is the absolute value of $h_1(q)$. Here $(x_f, y_f)$ and $R$ are constants and $x_l$ and $y_l$ are related to the state variables, $x_c$, $y_c$, and $\phi$, by Equations (34) and (35). The forward velocity of the platform is given by

$$h_2(\nu) = \dot{x}_c \cos\phi + \dot{y}_c \sin\phi = \frac{r}{2}(\nu_1 + \nu_2) \tag{47}$$

It is clear that we have a Type IV output. The decoupling matrix for this output equation is computed as follows.

$$\begin{aligned} \dot{y}_1 &= \frac{\partial h_1}{\partial x}\dot{x} = J_{h_1}(q)S(q)\nu \\ \ddot{y}_1 &= \frac{\partial (J_{h_1}S\nu)}{\partial q}S(q)\nu + J_{h_1}(q)S(q)u \\ \dot{y}_2 &= J_{h_2}u \end{aligned}$$

where

$$J_{h_1}(q) = \frac{\partial h_1}{\partial q} = \frac{1}{d_c}\begin{bmatrix} x_c - x_f + L\cos\phi \\ y_c - y_f + L\sin\phi \\ L\cos\phi(y_c - y_l) - L\sin\phi(x_c - x_f) \\ 0 \\ 0 \end{bmatrix}^T$$

$$J_{h_2} = [\frac{r}{2} \quad \frac{r}{2}]$$

$$d_c = \sqrt{(x_l - x_f)^2 + (y_l - y_f)^2}$$

Therefore, the decoupling matrix is

$$\Phi = \begin{bmatrix} J_{h_1}(q)S(q) \\ J_{h_2} \end{bmatrix} \tag{48}$$

and the determinant of $\Phi$ is

$$\det(\Phi) = \frac{rc(d+L)}{d_c}((y_c - y_f)\cos\phi - (x_c - x_f)\sin\phi)$$

It follows that the decoupling matrix is singular if (1) $L = -d$ (point $P_l$ coincides with point $P_o$), or (2) $(y_c - y_f)\cos\phi = (x_c - x_f)\sin\phi$ ( the heading direction of the platform or the $X$-axis is normal to the circular path). While the first condition is due to the nonholonomic constraint of the platform, and the second condition is due to the fact that the direction along the path is not explicitly specified in the function $h_1(q)$. Thus when the $X$-axis is normal to the path, specifying the forward velocity does not uniquely specify the path direction. We also note that in order to avoid this type of singularity it is beneficial to have $L > -d$ if the forward velocity is positive. Motion in the reverse direction can be accomplished with $L < -d$ and a negative forward velocity.

We now consider a straight line path. Let the path be described by $Ax + By + C = 0$.

$$h_1(x_c, y_c, \phi) = \frac{Ax_l + By_l + C}{\sqrt{A^2 + B^2}} \tag{49}$$

Once again, the shortest distance from point $P_l$ to the path is the absolute value of $h_1$. The second component of the output equation, $h_2$, is the same as for the circular path. The decoupling matrix $\Phi$ has the same form except that $J_{h_1}$ is now replaced by

$$J_{h_1} = \frac{1}{\sqrt{A^2 + B^2}} \begin{bmatrix} A \\ B \\ BL\cos\phi - AL\sin\phi \\ 0 \\ 0 \end{bmatrix}^T$$

The determinant of $\Phi$ is

$$\det\Phi = \frac{rc(d+L)}{\sqrt{A^2 + B^2}}(B\cos\phi - A\sin\phi)$$

Once again, the decoupling matrix is singular if $L = -d$ or the $X$-axis is perpendicular to the straight line path.

More generally, if $f(x, y) = 0$ is an arbitrary path, solving the shortest distance from point $P_l$ to the path involves solving the extremization problem

$$\min_{x,y} \left\{\frac{1}{2}((x - x_l)^2 + (y - y_l)^2) + \lambda^T f(x, y)\right\}$$

A closed form solution is impossible in a general case. However, an approximate expression for $h_1$ may be used instead:

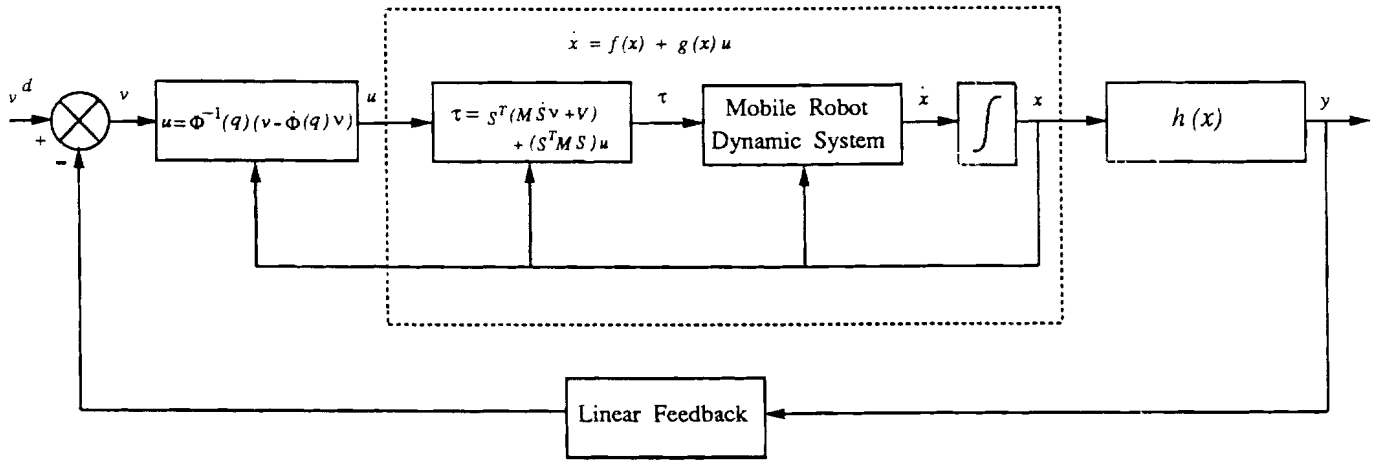


Figure 5: Schematic of the control algorithms

$$h_1 = f(x_l, y_l) \tag{50}$$

Although $h_1$ in this case is not the true distance to the path, it is a measure of the closeness to the given path. In the two basic paths discussed above, it is noted that the distance representation differs from the path descritiption only by a constant. Finally, we note that Dubins [8] and later Reeds and Shepp [18] showed that given any initial and final position and orientation of a car, there exists a family of paths composed of only straight line and circular arc segments between any two points. In fact, Dubins proved that this family contains the R-geodesic[6] between the two points. We use this result to argue that any path can be suitably broken down into straight line and circular arc segments. Therefore if we are able to control the mobile platform on such basic paths and on piecewise continuous paths composed of these two , we can effectively move from any position and orientation to any other position and orientation.

For either of the two basic paths or arbitrary path, by applying the nonlinear feedback, Equation (20), we obtain a linearized and decoupled system in the form

$$\ddot{y}_1 = v_1 \tag{51}$$

$$\dot{y}_2 = v_2 \tag{52}$$

A linear feedback can be designed to make each subsystem stable and to meet the performance specifications (see [26, 28], for example).

### 3.5 Design of the Control Algorithms

We presented two types of control algorithms for mobile robots: (a) trajectory tracking; (b) path following. While they differ in the selection of output equations, the basic scheme is the same as shown in Figure 5. In the figure, $v^d$ is the reference (desired) values for the outputs, $h_1$ and $h_2$. The nonlinear feedback (Equation (12)) cancels the nonlinearity in the dynamics so that the state equation is simplied into the form of Equation (13). This is represented by the dotted block in Figure 5. Note that the nonlinearity in the kinematics remains in the simplified state equation. A second

[6] An R-geodesic is the minimal length path between two points having an average curvature everywhere less than or equal to $R^{-1}$, where $R$ is a fixed positive number.

nonlinear feedback (Equation (20)) linearizes and decouples the input-output map. The overall system is thus decoupled into two linear subsystems. For trajectory tracking, both subsystems are of second order. In the case of path following, the distance control subsystem is of second order, and the velocity control subsystem is of first order. To stabilize these subsystems and to achieve the desired performance, an outer linear feedback loop is designed to place the poles of the system.

# 4 Evaluation of Control Schemes

## 4.1 The Dynamic Simulation

We developed a computer simulation in order to verify the validity of the dynamic model and the effectiveness of the control algorithm discussed in the previous sections for a mobile platform that is kinematically similar to the LABMATE. The dimensions and the inertial parameters are representative of the LABMATE platform. According to the notation introduced before :

$b$ = 0.75m;
$d$ = 0.30m;
$a$ = 2.00m;
$m_c$ = 30.00kg;
$m_w$ = 1.00kg;
$I_c$ = $15.625 kg\text{-}m^2$;
$I_w$ = $0.005 kg\text{-}m^2$;
$I_m$ = $0.0025 kg\text{-}m^2$.

The virtual reference point $P_l$ was chosen to be coincident with $P_c$. The gains for the linear outer loop were designed in such a way that we got an overdamped system for the decoupled position control subsystem. This is appropriate if we want to follow a wall or a path with a median or a divider. In such a case the platform should not overshoot its desired path. On the other hand, we can choose a critically-damped system if we want to follow a curve on the middle of the road.

## 4.2 Trajectory tracking versus dynamic path following

Consider a straight line path, $y = x$, as shown in Figures 6 and 1. The reference point is defined so that $L = 0.0$ meters. The initial position is such that

$$(x_c, y_c) = (x_l, y_l) = (0.8, 0.2)$$

and the initial velocity is zero. The desired forward velocity is 1.414 m/sec. For the trajectory tracking algorithm,

$$h_1 = x_l, \quad h_2 = y_l$$
$$v_1^d = t, \quad v_2^d = t$$

For the path following algorithm,

$$h_1 = \frac{1}{\sqrt{2}}(y_l - x_l), \quad h_2 = \frac{r}{2}(\nu_1 + \nu_2)$$

$$v_1^d = 0, \quad v_2^d = 1.414$$

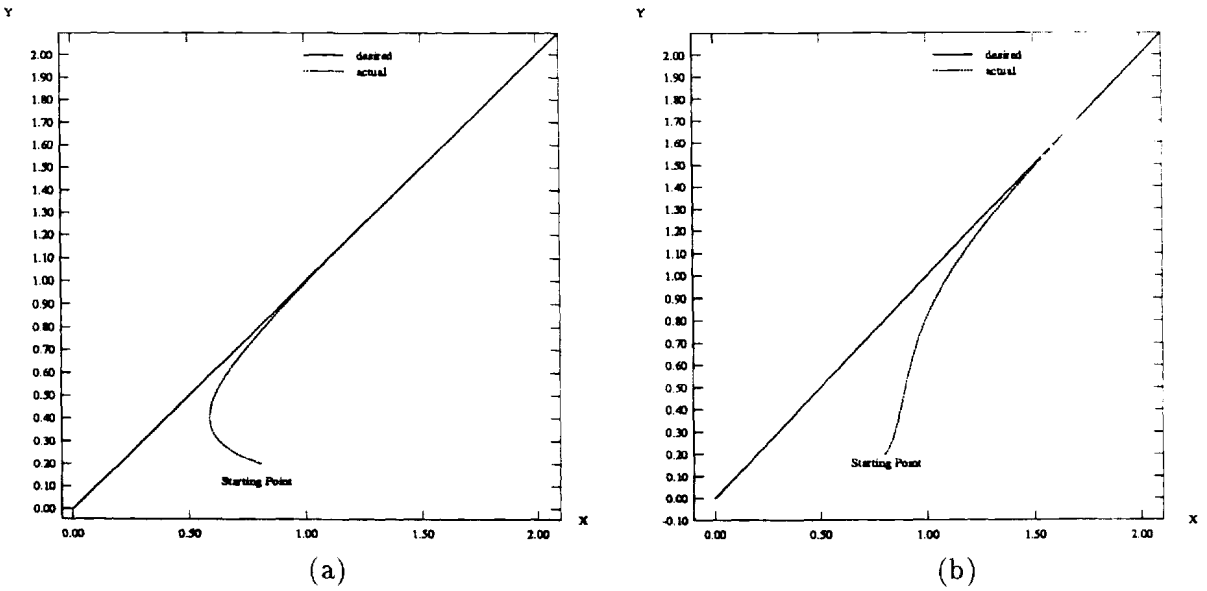


Figure 6: (a) Trajectory and (b) path of a reference point on a wheeled vehicle.

In both cases, as shown in Figure 6 the reference point is able to reach the path and stay on the path. Note that the gains for the position variables are same for both cases. The path following algorithm seems to exhibit a gradual merge while the trajectory tracking reacts more quickly and, depending on the gains, it even forces the reference point in the wrong direction. Depending on the point of interest, the trajectory tracking algorithm also results in cusps in the trajectory. For example, consider the locus of the geometric center, $P_o$, in both cases for different desired forward velocities as shown in Figures 1 . With a Type IV output equation the actual path followed is smooth but the Type I output equation often produces a discontinuity in the slope of the trajectory. This can also be seen from the velocity history shown in Figure 7. In this figure we have shown the forward velocity corresponding to case C of Figure 1. With the Type IV output equation the forward velocity exhibits a smooth exponential response that is typical of a first order system as expected (Figure 7 (b)). The trajectory tracking algorithm may result in discontinuities in velocities. As shown in Figure 7 (a), the center of the vehicle is accelerated and then decelerated to a stop twice before monotonically increasing to the desired velocity. If the objective is to follow a desired path, as is the case in autonomous navigation [20], it is clear that the path following algorithm is more appropriate. It is possible that trajectory tracking may be desirable in applications in which time is a critical parameter. It appears that for a wide range of applications in robotics that path following is the more appropriate strategy. For this reason, from this point on, we concentrate on Type IV output equations. The results of numerical experiments with path following algorithms are presented in the remainder of this section.

## 4.3 Performance of dynamic path following algorithms

### 4.3.1 Effect of initial conditions

The initial condition that most affects the trajectory is the initial velocity. Hence the two most important parameters are the initial heading angle ($\phi$) and the magnitude of the initial forward

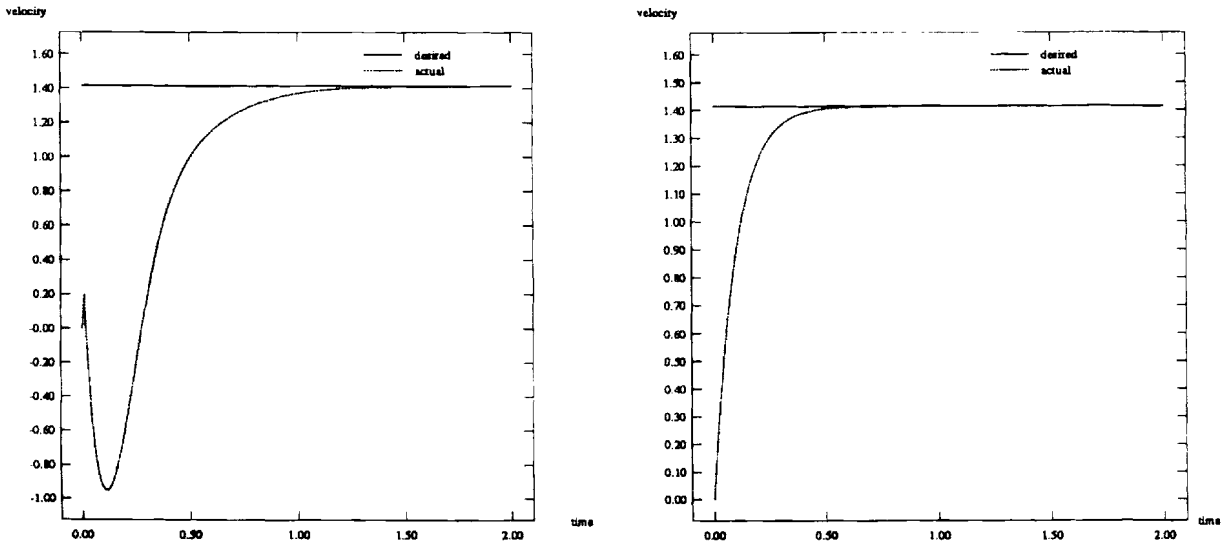


Figure 7: Forward velocity of the geometric center $P_o$ in (a) trajectory tracking ; (b) path following.

velocity. Figure 8 (a) shows how the mobile platform follows a circular path when it starts with a forward velocity of 5m/s but with different initial heading angles ($\phi$). Here the initial reference point position is

$$(x_l, y_l) = (30.0, 15.0)$$

and

$$h_1(q) = ((x_l - 20.0)^2 + (y_l - 20.0)^2)^{1/2} - 10.0, \qquad h_2 = \frac{r}{2}(\nu_1 + \nu_2)$$

$$v_1^d = 0, \qquad v_2^d = 1.414$$

We note that the algorithm is singular if the vehicle is oriented along the shortest line joining the reference point and the path. In this case an orientation with $\phi = -26.6$ deg or 153.4 deg leads to problems. For heading angles other than these, the response is satisfactory as seen from the Figure 8 (a).

Figure 8 (b) depicts the system response for a desired circular path for different initial forward velocities but with a constant heading angle (in this case it was 0 degrees). As expected, if the initial heading is away from the desired path (as in this case), the system exhibits better performance when the initial speed is less.

### 4.3.2 Effect of modeling uncertainties

Modeling errors can result due to the difficulty in measuring or estimating the geometric, kinematic or inertial parameters or from the lack of a complete knowledge of the components of the system. We simulated modeling errors in the inertial parameters namely $m_c$ and $m_w$ and investigated the performance on a straight line path as well as on a circular path. For as much as a 100 percent modeling error in $m_c$ and $m_w$, the control scheme follows the path quite well. Although a theoretical robustness analysis was not performed, it appears from extensive simulations that the scheme is quite robust. Figures 9 (a) and (b) shows the response of the system for a straight line and circular

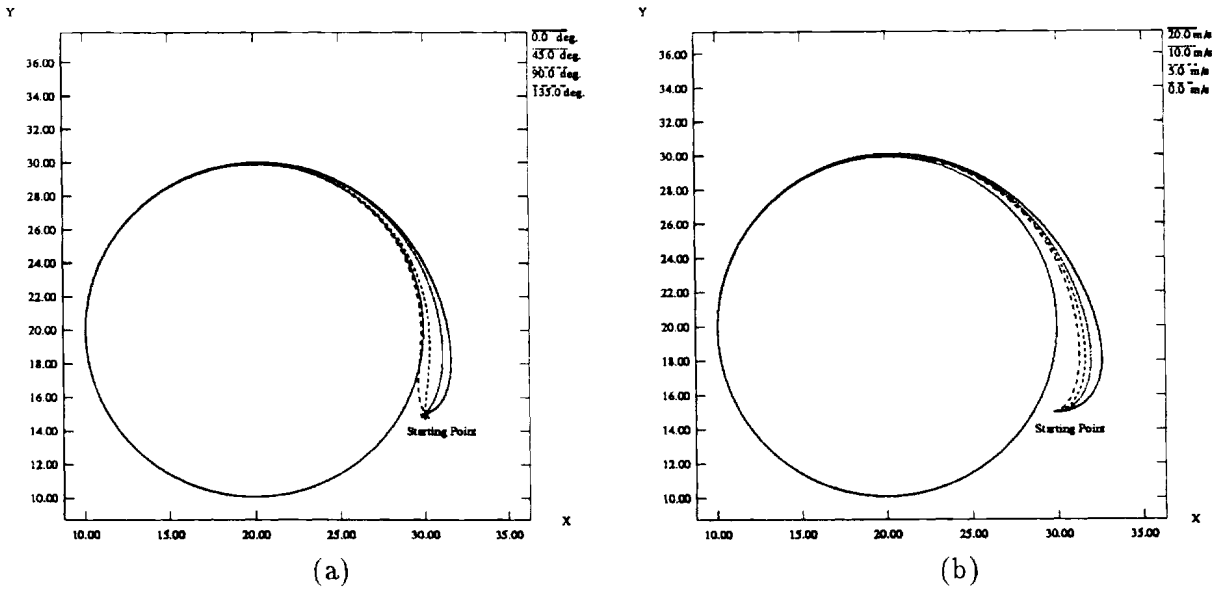


Figure 8: Path followed with : (a) different initial heading angles (in degrees) for an initial forward velocity of 5 meters/sec; (b) different initial forward velocities in (meters/sec) for an initial heading angle of 0 degrees.

path respectively. It takes a longer time in comparison to the case when there is no modelling error (as seen from the path C of Figure 1 (b)), to converge to the desired path for a straight line path whereas it follows the circular path but only with a small constant offset.

### 4.3.3 Piecewise continuous paths

It is shown in References [8] and [18] that the shortest paths for wheeled mobile carts are composed of circular arcs and straight lines. The result is a piecewise continuous path with discontinuities in the curvature and higher derivatives. An example[7] of such a path is shown in Figure 10 where A and C are circular arcs and B is a straight line. The performance of the control system is shown in Figure 11 . The magnified view of the first transition point in Figure 12 shows that the performance is acceptable — discontinuities in curvature are negotiated without any difficulty. We note that the second transition involves a smaller change in curvatures since arc $C$ possesses a smaller radius of curvature. As a result there is almost no deviation of the actual path from the desired one.

## 4.4 A recalibration scheme for mobile robots

In wheeled vehicles, there is no direct way of obtaining position feedback. The position (and orientation) of the vehicle may be estimated from the positions or velocities of the wheels. There may be small errors in the estimates either due to slippage and scuffing or due to errors in the wheel sensors. Since small errors in the angular velocities integrated over a large time interval result in large position errors, this presents a serious problem in control.

[7]Note that the discussion in References [8] and [18] is limited to circular arcs of constant curvature. Here, we consider different curvatures in order to investigate the effect of changing curvature.

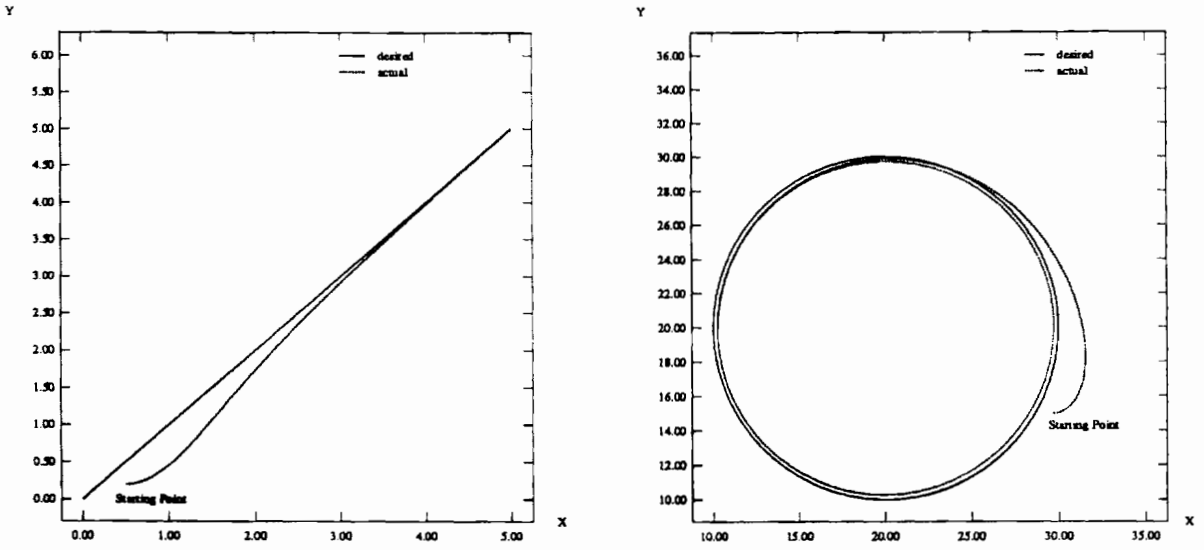


Figure 9: Desired and actual path of the mobile platform when there is a modeling error in $m_c$ and $m_w$ by 100% for the case of a : (a) straight line ; (b) circle.

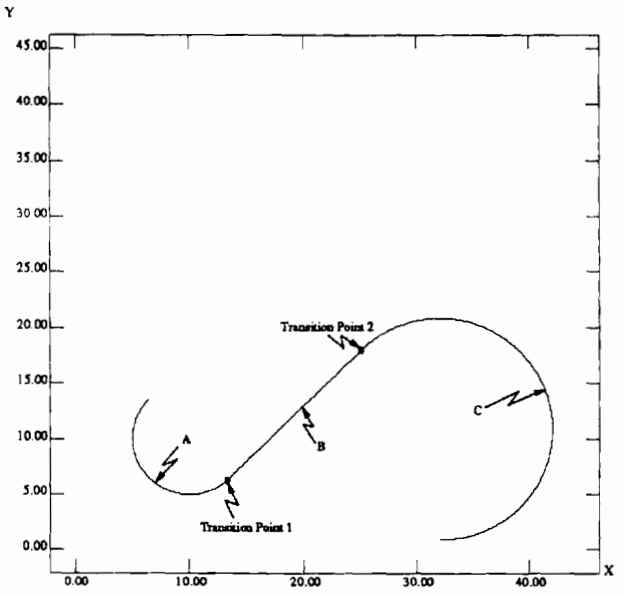


Figure 10: Desired composite path.

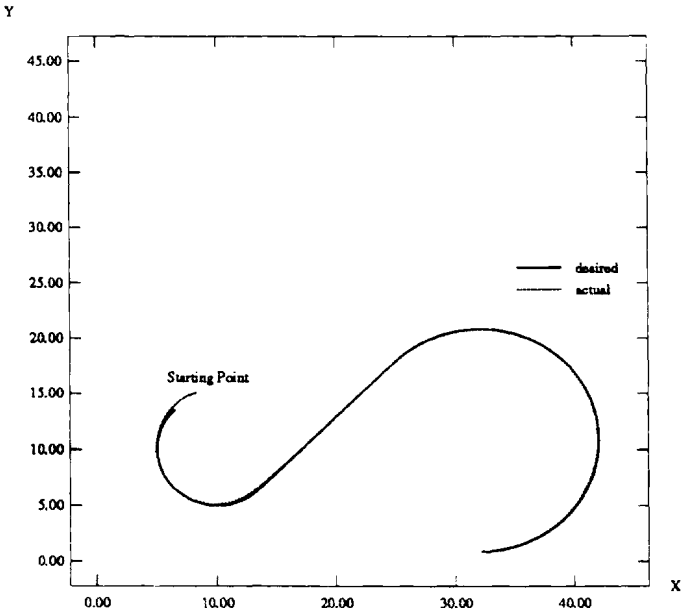


Figure 11: Performance of the platform in composite path following.

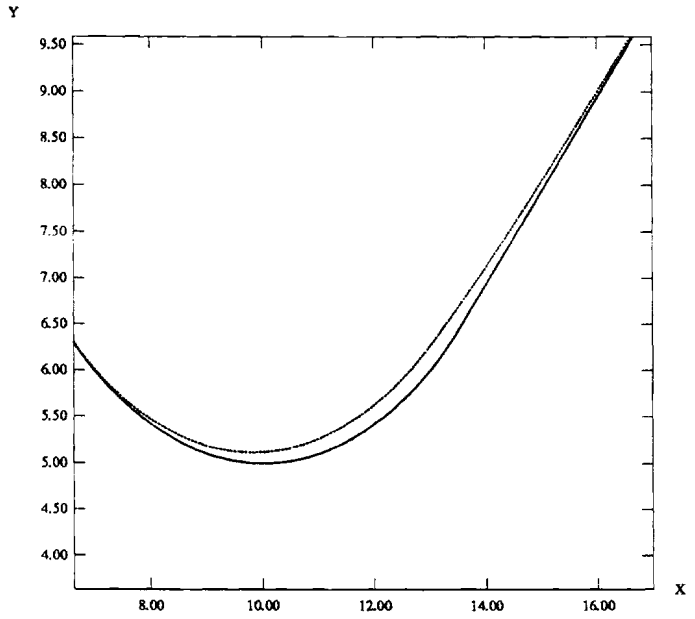


Figure 12: Magnified view of the first transition point in Figure 11.

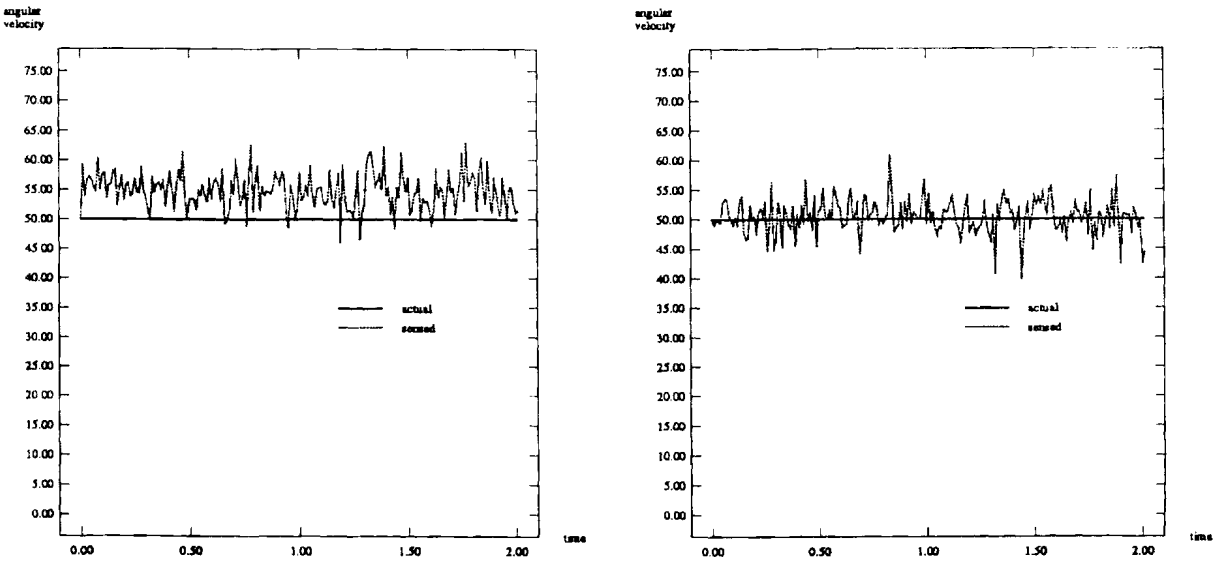


Figure 13: Sensory noise in the measurement of the angular velocity of : (a) the right wheel ; (b) the left wheel.

We consider a situation in which the sensed wheel angular velocities are different from the actual angular velocities. We generated noise using Gaussian distribution and simulated the sensed angular velocities as follows:

$$(\dot{\theta}_r)^{sensed} = (\dot{\theta}_r)^{actual} + (\dot{\theta}_r)^{noise} \quad (53)$$

$$(\dot{\theta}_l)^{sensed} = (\dot{\theta}_l)^{actual} + (\dot{\theta}_l)^{noise} \quad (54)$$

where $(\dot{\theta}_r)^{noise}$ and $(\dot{\theta}_l)^{noise}$ are random signals. The mean and standard deviation of $(\dot{\theta}_r)^{noise}$ are 5.0 radian/sec and 3.0 radian/sec respectively and that of $(\dot{\theta}_l)^{noise}$ are 0.5 radian/sec and 3.0 radian/sec respectively.

This is shown in Figures 13 (a) and (b) for a uniform straight line motion. The performance of the control system is shown in Figure 14 for a circular path. It is evident that the vehicle's path diverges from the desired path. However from the "sensed path" shown in the figure it is clear that the vehicle "thinks" that it is close to the desired path. The only remedy to this problem is to provide some form of end-point feedback.

In Figures 15 and 16 we consider end-point feedback at rates that are much lower than servo-level sampling rates. If end-point feedback is available once every second, the path (shown in Figure 15) exhibits a significant improvement (compared to Figure 14). Note that while the sensed position exhibits a discontinuity, the actual position and velocity are not discontinuous. The performance improves with increased end-point feedback frequency as shown in Figure 16 for a 2 Hz. sampling rate. In practice, vision systems are capable of providing frame-rates that are well above 10 Hz. [5].

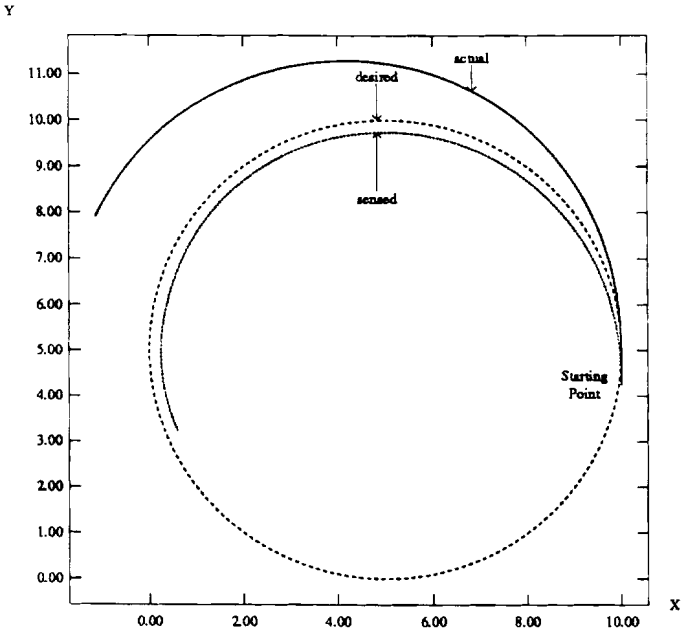


Figure 14: Effect of sensory noise on the performance of the mobile platform.

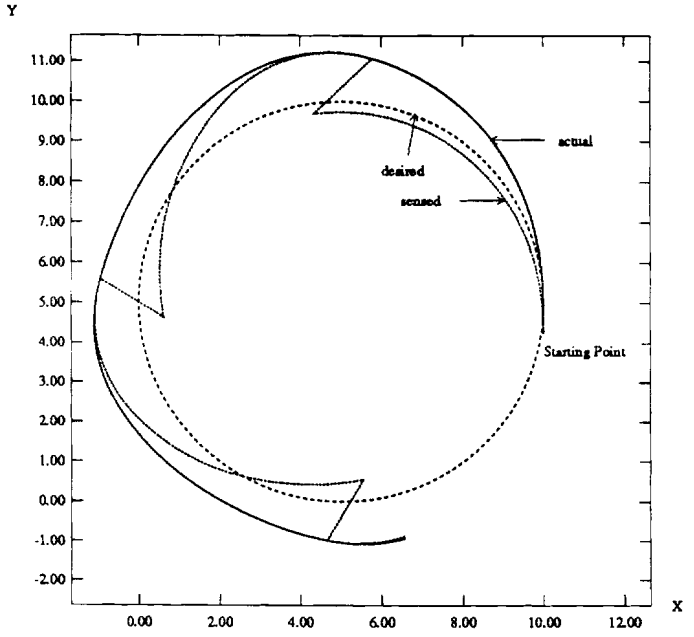


Figure 15: Effect of recalibration on the actual path followed by the platform when the recalibration frequency is 1 Hz.

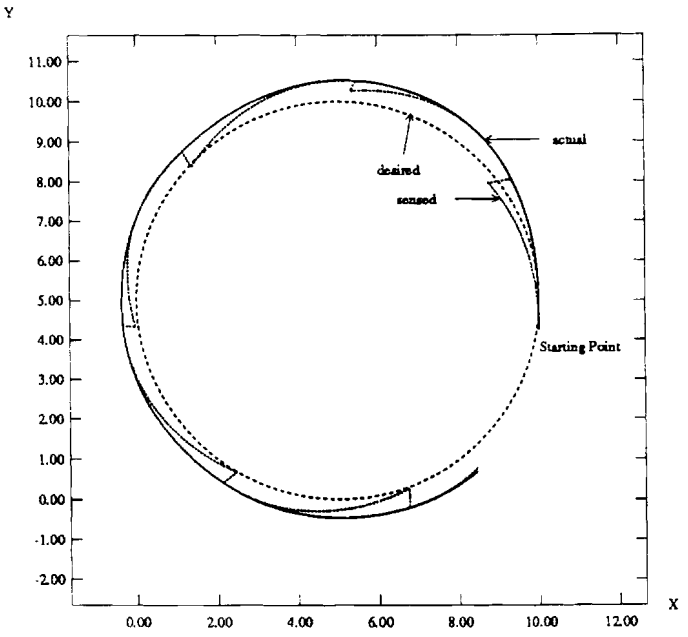


Figure 16: Effect of recalibration on the actual path followed by the platform when the recalibration frequency is 2 Hz.

# 5 Conclusion

We have presented a general method of controlling mechanical systems with holonomic as well as nonholonomic constraints. We discussed the input-output linearization and the zero dynamics of such systems. For wheeled mobile platforms, we derived a nonlinear feedback that guarantees input-ouput stability and Lagrange stability for the overall system. We investigated two types of control algorithms: trajectory tracking and path following. The dynamic path following problem was presented here for the first time. Computer simulation results were presented to illustrate and compare the performance of each algorithm. Based on these it was concluded that a dynamic path-following scheme is more appropriate for vehicle control applications. Finally, the effects of modelling errors and sensor noise are investigated through numerical experiments.

# 6 Acknowledgement

This work was in part supported by: Airforce grant AFOSR F49620-85-K-0018, Army/DAAG-29-84-K-0061, NSF-CER/DCR82-19196 Ao2, NASA NAG5-1045, ONR SB-35923-0, NIH grant NS-10939 -11 as part of Cerebro Vascular Research Center, NIH 1-RO1-NS-23636-01, NSF INT85-14199, NSF DMC85-17315, NSF CISE/CDA-90-2253, NSF MSS-91-57156, ARPA N0014-88-K-0632, NATO grant No. 0224/85, DEC Corp., and IBM Corp.

## References


[1] J. Barraquand and Jean-Claude Latombe. Nonholonomic multibody mobile robots: controllability and motion planning in the presence of obstacles. In *Proceedings of 1991 International Conference on Robotics and Automation*, pages 2328–2335, Sacramento, CA, April 1991.

[2] Anthony Bloch and N. H. McClamroch. Control of mechanical systems with classical nonholonomic constraints. In *Proceedings of 28th IEEE Conference on Decision and Control*, pages 201–205, Tampa, Florida, December 1989.

[3] Anthony Bloch, N. H. McClamroch, and M. Reyhanoglu. Controllability and stability properties of a nonholonomic control system. In *Proceedings of 29th IEEE Conference on Decision and Control*, pages 1312–1314, Honolulu, Hawaii, December 1990.

[4] G. Campion, B. d'Andrea-Novel, and G. Bastin. Controllability and state feedback stabilization of non holonomic mechanical systems. In C. Canudas de Wit, editor, *Lecture Notes in Control and Information Science*, pages 106–24, Springer-Verlag, 1991.

[5] James J. Clark and Nicola J. Ferrier. Control of visual attention of mobile robots. In *IEEE International Conference on Robotics and Automation*, pages 826–831, May 1989.

[6] B. d'Andrea-Novel, G. Bastin, and G. Campion. Modelling and control of non holonomic wheeled mobile robots. In *Proceedings of 1991 International Conference on Robotics and Automation*, pages 1130–1135, Sacramento, CA, April 1991.

[7] C. Canudas de Wit and R. Roskam. Path following of a 2-DOF wheeled mobile robot under path and input torque constraints. In *Proceedings of 1991 International Conference on Robotics and Automation*, pages 1142–1147, Sacramento, CA, April 1991.

[8] L. E. Dubins. On curves of minimal length with a constraint on average curvature, and with prescribed initial and terminal positions and tangents. *American Journal of Mathematics*, 79:497–516, 1957.

[9] T. Fraichard. Smooth trajectory planning for a car in a structured world. In *Proceedings of 1991 International Conference on Robotics and Automation*, pages 318–323, Sacramento, CA, April 1991.

[10] Y. Koren and J. Borenstein. Potential field methods and their inherent limitations for mobile robot navigation. In *Proceedings of 1991 International Conference on Robotics and Automation*, pages 1398–1404, Sacramento, CA, April 1991.

[11] V. Kumar and K. J. Waldron. Actively coordinated vehicle systems. *ASME Journal of Mechanisms, Transmissions, and Automation in Design*, 111, June 1989.

[12] V. Kumar and K.J. Waldron. Force distribution in walking vehicles. *ASME Journal of Mechanical Design*, July 1990.

[13] V. Kumar, X. Yun, E. Paljug, and N. Sarkar. Control of contact conditions for manipulation with multiple robotic systems. In *Proceedings of 1991 International Conference on Robotics and Automation*, Sacramento, CA, April 1991.

[14] J. P. Laumond. Finding collision-free smooth trajectories for a non-holonomic mobile robot. In *10th International Joint Conference on Artificial Intelligence*, pages 1120–1123, Milano, Italy, 1987.

[15] David J. Montana. The kinematics of contact and grasp. *The International Journal of Robotics Research*, 7(3):17–32, June 1988.

[16] H. Nijmeijer and A. J. van der Schaft. *Nonlinear Dynamic Control Systems.* Springer-Verlag, New York, 1990.

[17] L. A. Pars. *A Treatise on Analytical Dynamics.* Wiley, New York, 1968.

[18] J. A. Reeds and L. A. Shepp. Optimal paths for a car that goes both forwards and backwards. *Pacific Journal of Mathematics*, 145(2):367–393, 1990.

[19] C. Samson and K. Ait-Abderrahim. Feedback control of a nonholonomic wheeled cart in cartesian space. In *Proceedings of 1991 International Conference on Robotics and Automation*, pages 1136–1141, Sacramento, CA, April 1991.

[20] S. Singh, D. Feng, P. Keller, G. Shaffer, W. F. Shi, D. H. Shin, J. West, and B. X. Wu. *A System for Fast Navigation of Autonomous Vehicles.* Technical Report CMU-RI-TR-91-20, The Robotics Institute, Carnegie Mellon University, Pittsburgh, Pennsylvania, September 1991.

[21] S. Singh and P. Keller. Obstacle detection for high speed autonomous navigation. In *Proceedings of 1991 International Conference on Robotics and Automation*, pages 2798–2805, Sacramento, CA, April 1991.

[22] T. Skewis, J. Evans, V. Lumelsky, B. Krishnamurthy, and B. Barrows. Motion planning for a hospital transport robot. In *Proceedings of 1991 International Conference on Robotics and Automation*, pages 58–63, Sacramento, CA, April 1991.

[23] Jean-Jacques E. Slotine and Weiping Li. *Applied Nonlinear Control.* Prentice Hall, Inc., Englewood Cliffs, New Jewsey, 1991.

[24] T. Yoshikawa. Dynamic hybrid position/force control of robot manipulators — description of hand constraints and calculation of joint driving force. *IEEE Journal of Robotics and Automation*, RA-3(5):386–392, October 1987.

[25] X. Yun, V. Kumar, N. Sarkar, and E. Paljug. Control of multiple arm systems with rolling constraints. In *IEEE International Conference on Robotics and Automation*, May 1992.

[26] Xiaoping Yun. Dynamic state feedback control of constrained robot manipulators. In *Proceedings of the 27th IEEE Conference on Decision and Control*, pages 622–626, Austin, Texas, December 1988.

[27] Xiaoping Yun, Vijay Kumar, Nilanjan Sarkar, and Eric Paljug. *Control of Multiple Arm Systems with Rolling Constraints.* Technical Report MS-CIS-91-79, GRASP LAB 278, Department of Computer and Information Science, University of Pennsylvania, Philadelphia, PA 19104, 1991.

[28] Xiaoping Yun and Vijay R. Kumar. An approach to simultaneous control of trajectory and interaction forces in dual arm configurations. *IEEE Transactions on Robotics and Automation*, 7(5):618–625, October 1991.